Preparation of porous tin dioxide powder by ultrasonic spray pyrolysis and their application to sensor materials

Koji Hieda, Takeo Hyodo, Yasuhiro Shimizu and Makoto Egashira*
Department of Materials Science and Engineering, Faculty of Engineering, Nagasaki University
1-14 Bunkyo-machi, Nagasaki 852-8521, Japan
*egashira@nagasaki-u.ac.jp

Abstract

Porous SnO_2 powders have been prepared by pyrolysis of atomized aqueous $SnCl_2$ or $SnCl_4$ precursor solutions containing polymethylmethacrylate (PMMA) microspheres. The diameter of macropores existing in the porous SnO_2 powders (about 400~800 nm in diameter) was about 150~200 nm. In addition, the wall thickness of the porous SnO_2 powder prepared from $SnCl_2$ was presumed to be thinner than that prepared from $SnCl_4$. A SnO_2 sensor fabricated from the powder prepared by pyrolysis of the aqueous $SnCl_2$ solution at 1100°C showed the highest response to 1000 ppm H_2 in air among the sensors tested.

1. Introduction

SnO_2 is well-known as the most important material for semiconductor gas sensors because of its relatively high gas sensing properties as well as high chemical stability [1, 2]. For further improvement of the gas sensitivity and selectivity, however, strict control of gas reactivity and selectivity is indispensable. Therefore, we have so far demonstrated the optimization of nano- and micro-structure of the sensors by utilizing various techniques. For example, the introduction of ordered mesoporous structure into SnO_2 powder was found to be very effective for controlling the gas diffusivity and reactivity [3-6]. Chemical surface modification of SnO_2 powder with some kinds of alkoxysilanes was also found to be very promising as a technique for getting high performance sensors, because the gas diffusivity and potential barrier height among SnO_2 grains could be controlled precisely [7-10]. In addition, it was revealed that anodically oxidized titania films coupled with a palladium electrode were potential diode-type H_2 sensor materials with a Schottky barrier at the palladium-oxide interface [11-14].

By the way, an ultrasonic spray pyrolysis method is one of the effective techniques for preparing highly dispersed oxide powders. Recently, we have succeeded to prepare submicron-size hollow alumina microspheres with controlled thickness and crystal structure [15, 16]. It is worth noting that Iskandar et al. have prepared various kinds of oxide microspheres involving macropores by thermal decomposition of atomized oxide precursor solutions containing submicron-sized polystyrene microspheres as a template [17, 18]. The introduction of macropores into the constituent materials for some electrochemical devices such as fuel cells and chemical sensors is very important to improve their performance, because reactants and products of the electrochemical reactions should be diffused or transferred easily through the macropores. Actually, we have demonstrated that well-developed macroporous ceramic films, which were prepared by a modified sol-gel technique by employing polymetheylmethacrylate (PMMA) microspheres as a template, showed excellent sensing properties to H_2 and NO_x [19-21].

In this study, therefore, attempts have been made to prepare porous SnO_2 powders by pyrolysis of atomized aqueous precursor solutions containing PMMA microspheres. Then, potential of these porous SnO_2 powders as a new sensor material has been examined.

2. Experimental

2.1. Preparation of porous SnO_2 powder by ultrasonic spray pyrolysis method

PMMA microspheres (Soken Chem. & Eng. Co., Ltd., 250 nm in diameter) of 0.5 g were added to 0.05 mol dm^{-3} $SnCl_2$ or $SnCl_4$ aqueous solutions of 100 ml, and the mixtures were served as precursor solutions for preparation of porous SnO_2 powders by ultrasonic spray pyrolysis. In some cases, $SbCl_3$ was also added to the mixtures at a level of 0.1 wt% of the weight of $SnCl_2$ or $SnCl_4$ in order to improve the conductivity of resultant SnO_2 powder. We used a flow spray pyrolysis system equipped with a specially designed mist-supply to prepare porous SnO_2 powder in an electric furnace, as shown in Fig. 1. The mist of the precursor solutions was generated in a plastic container equipped with a polyethylene thin film at one end, which was set perpendicular over an ultrasonic vibrator (Honda Electric Co., Ltd., HM-303N, 2.4 MHz) at a distance of 0.5~1.0 cm in water. And then, the mist was carried into a glass vessel by air flowing 1 (1.5 dm^3 min^{-1}), and only small droplets were allowed to move into an electric furnace heated at 800~1100°C with a help of air flowing 2 (1.5 dm^3 min^{-1}). Porous SnO_2 powders obtained were characterized by transmission electron microscopy (TEM), scanning electron microscopy (SEM) and X-ray diffraction analysis (XRD). Porous SnO_2 (pr-SnO_2, pr means “porous”) powders prepared by $SnCl_2$ and $SnCl_4$ solutions are denoted as pr-SnO_2(n)T in this

study (n: raw material, d for $SnCl_2$ and t for $SnCl_4$, respectively, and T: the calcination temperature (800~1100°C)). In addition, Sb-doped SnO_2 is referred to as pr-Sb/SnO_2(n)T. For comparative purpose, a conventional SnO_2 (c-SnO_2) powder was prepared by pyrolysis of tin oxalate at 600°C for 5 h.

2.2. Fabrication of sensors and their hydrogen sensing properties

Thick film sensors were fabricated by applying the paste of pr-SnO_2(n)T, pr-Sb/SnO_2(n)T or c-SnO_2 powder on alumina substrates equipped with a pair of interdigitated Pt electrodes, followed by calcination at 550°C for 5 h. Gas responses of these sensors were measured to 1000 ppm H_2 balanced with air in a flow apparatus at 250~500°C. Sensor response was defined as the ratio (R_a/R_g) of sensor resistance in air (R_a) to that in H_2 balanced with air (R_g).

3. Results and discussion

3.1. Characterization of pr-SnO_2(n)T and pr-Sb/SnO_2(n)1100 powders

XRD patterns of four kinds of pr-SnO_2(d)T and pr-SnO_2(t)1100 powders are shown in Fig. 2. All specimens exhibited casserite-type structure, while the crystallite size (CS) of the pr-SnO_2(d)T powder calculated by the Scherrer equation increased with a rise in pyrolysis temperature. In addition, the kind of Sn-source seems to have a large influence on the value of CS. Namely, the crystallite size of pr-SnO_2(t)1100 fabricated from $SnCl_4$ was much larger than that of pr-SnO_2(d)1100 fabricated from $SnCl_2$.

TEM images of pr-SnO_2(d)T (T = 800~1100) and pr-SnO_2(t)1100 are shown in Fig. 3. Many macropores replicating the shape of submicron-size PMMA microspheres (d: 250 nm) were observed in all the resultant porous SnO_2 particles. The diameter of macropores existing in the porous SnO_2 powder (about 400~800 nm in diameter), about 150~200 nm, was slightly reduced from that of PMMA microspheres. Formation of such spherical macropores may suggest the slower pyrolysis rate of PMMA than that of tin chloride. In addition, we can see that the morphology of macropores is not dependent on the pyrolysis temperature, suggesting high thermal stability of the porous structure. Furthermore, it was revealed in high magnification TEM images that one granular particle consisted of many very fine particles. The mean particle sizes (PS) observed are indicated in Fig. 3. These values are well coincident with the crystallite sizes calculated by the Scherrer equation (see Fig. 2). Another notable finding is that the image of pr-SnO_2(t)1100 is much darker than that of pr-SnO_2(d)1100. The darker image may suggest thicker SnO_2 walls inside the granular particle. Furthermore, the particle size of pr-SnO_2(d)1100

(ca. 12.5 nm) was much smaller than that of pr-SnO_2(t)1100 (ca. 20.0 nm), in a similar manner to the order of crystallite size.

Pore size distribution and specific surface area (SSA) of pr-SnO_2(d)T (T = 800~1100) and pr-SnO_2(t)1100 are shown in Fig. 4. These specimens showed relatively smaller SSA than that of mesoporous SnO_2 powder prepared from Na_2SnO_3 as a tin source and cetyltrimethylchloride as a mesopore template (ca. 300 m^2 g^{-1} after calcination at 600°C for 5 h) [3, 4], because of the high pyrolysis temperature (800~1100°C). However, SSA of pr-SnO_2(d)T (T = 800~1100) was much larger than that of c-SnO_2 powder prepared by pyrolysis of tin oxalate at 600˚C for 5 h as a reference, whereas that of pr-SnO_2(t)1100 showed a much smaller SSA value. Specific surface area of three kinds of pr-SnO_2(d)T powders pyrolyzed at temperatures less than 1000˚C was almost comparable to each other, but pr-SnO_2(d)1100 showed the smallest surface area among the powders prepared from $SnCl_2$. This result may be explained by a decrease in the amount of pores with sizes of 2~4 nm in diameter. In addition, from the comparison between the pore size distribution and TEM images (Figs. 3(a)'~(d)'), we can understand that nanopores of less than about 4 nm reflect the spaces formed among crystallites, while mesopores of about 30 nm seem to correspond to the spaces formed among crystallite agglomerates. However, the larger SSA of pr-SnO_2(d)1100 than pr-SnO_2(t)1100 may reflect large amounts of nano (ca. 4 nm in diameter) and mesopores (ca. 30 nm in diameter), as shown in Fig. 4(d).

Figure 5 shows SEM images of typical thick films fabricated from pr-SnO_2(d)1100 and pr-SnO_2(t)1100. In the case of pr-SnO_2(d)1100 (Fig. 5(a)), formation of macropores at the surface of SnO_2 powder was obscure due to formation of many SnO_2 nanoparticles, which have already been observed around pr-SnO_2(d)1100 powder in Fig. 3(d). The morphology of other pr-SnO_2(d)n sensors was almost the same as that of pr-SnO_2(d)1100 shown in Fig. 5(a). In contrast, formation of macropores at the surface of pr-SnO_2(t)1100 powder having clear boundaries among them is obvious in Fig. 5(b), then little nanoparticles appear.

3.2. H_2 sensing properties of thick film pr-SnO_2(n)T sensors and the effects of Sb-doping to pr-SnO_2(n)1100

Typical response transients to 1000 ppm H_2 of pr-SnO_2(d)1100 and c-SnO_2 sensors are shown in Fig. 6. The pr-SnO_2(d)1100 sensor showed relatively slow response and recovery speeds and extremely high resistance in air, compared with those of c-SnO_2. However, the magnitude of response (R_a/R_g) of pr-SnO_2(d)1100 was much higher than that of c-SnO_2. Figure 7 shows operating temperature dependence of responses to 1000 ppm H_2 of four kinds of pr-SnO_2(d)T and c-SnO_2 sensors. The maximum R_a/R_g of the c-SnO_2 sensor was ca. 20 at 400˚C. On the other hand, pr-SnO_2(d)T sensors, fabricated from porous SnO_2 powders involving macropores,

showed larger H_2 response than the c-SnO_2 sensor, probably because porous SnO_2 powders had a large surface area, and then a large number of active sites. H_2 gas diffusion control may have been generated by such macroporous structure, and then have contributed to the enlargement of H_2 gas response. The R_a/R_g of pr-SnO_2(d)1100 (ca. 60 at 350˚C) showed the highest value among pr-SnO_2(d)T sensors, while it showed extremely high resistance in air (see Fig. 6(a)). As shown in Figs. 2 and 4, the pr-SnO_2(d)1100 sensor showed the largest crystallite size and the smallest specific surface area among pr-SnO_2(d)T sensors. These changes in microstrucutre induced by a rise in calcination temperature usually leads to a decrease in gas response. However, the fact that the largest response observed with the pr-SnO_2(d)1100 sensor implies the existence of other response determining factors, such as optimization of gas diffusivity and reactivity at the surface of sensor materials. Also in the case of the pr-SnO_2(t)1100 sensor fabricated from the $SnCl_4$ precursor solution, the H_2 response could not be measured due to its extremely high sensor resistance. Therefore, Sb-doping into the Sn sites of pr-SnO_2(n)1100 was attempted to decrease the sensor resistance in air.

Response transients of pr-Sb/SnO_2(d)1100 and pr-Sb/SnO_2(t)1100 sensors are shown in Fig. 8. The sensor resistance of pr-Sb/SnO_2(d)1100 could be reduced by two orders of magnitude by the Sb-doping. In addition, the response and recovery speeds could also be improved drastically, and they were faster than those of the c-SnO_2 sensor. In contrast, the resistance of the pr-Sb/SnO_2(t)1100 sensor in air could be decreased to a level capable of measuring, but it was still too high to be put into practical use, along with terribly slow response and recovery speeds.

However, the Sb-doping reduced the response to H_2. Operating temperature dependences of responses to 1000 ppm H_2 of the pr-Sb/SnO_2(d)1100 and pr-Sb/SnO_2(t)1100 sensors are shown in Fig. 9. For reference, the result of the c-SnO_2 sensor is cited again in Fig. 9. All the sensors showed good reproducibility in sensing properties within our laboratory test period. The response of the pr-Sb/SnO_2(d)1100 sensor was much smaller than that of the pr-SnO_2(d)1100 sensor and was comparable to that of the c-SnO_2 sensor. On the other hand, the pr-Sb/SnO_2(t)1100 sensor showed larger H_2 response than the c-SnO_2 sensor, but the extremely high resistance and terribly slow response and recovery speeds (Fig. 8(b)) are the problem. Further improvement of the sensor properties are now under investigation by various techniques such as strict control of the sensor nanostructure, surface modification and noble-metal doping.

4. Conclusion

Porous SnO_2 powders (the diameter: 400~800 nm, spherical pore diameter: 150~200 nm) have been prepared by pyrolysis of atomized aqueous $SnCl_2$ or $SnCl_4$ precursor solutions containing PMMA microspheres. The morphology of macropores replicating the shape of submicron-size PMMA microspheres was found to be less dependent on the pyrolysis temperature, suggesting high thermal stability of the porous structure. Specific surface area of pr-SnO_2(d)T (T = 800~1100) was much larger than that of pr-SnO_2(t)1100. In addition, SEM images of pr-SnO_2(d)1100 showed that macropores were obscure at the surface of SnO_2 powder due to formation of many SnO_2 nanoparticles. In contrast, formation of macropores at the surface of p-SnO_2(t)1100 powder having clear boundaries among them was observed clearly, probably due to less formation of nanoparticles.

The R_a/R_g of pr-SnO_2(d)1100 (ca. 60 at 350˚C) showed the highest value among pr-SnO_2(d)T sensors, while it showed extremely high resistance in air. Sb-doping into the Sn sites of pr-SnO_2(n)1100 was attempted to decrease the sensor resistance in air. As a result, sensor resistance and H_2 response decreased, but response and recovery speeds of the pr-SnO_2(d)1100 sensor drastically improved.

References

1. N. Yamazoe, New approaches for improving semiconductor gas sensors, Sens. Actuators B 5 (1991) 7-19.
2. Y. Shimizu, M. Egashira, Basic aspects and challenges of semiconductor gas sensors, MRS Bull. 24 (1999) 18-24.
3. T. Hyodo, N. Nishida, Y. Shimizu, M. Egashira, Preparation and gas-sensing properties of thermally stable meesoporous SnO_2, Sens. Actuators B 83 (2002) 209-215.
4. T. Hyodo, S. Abe, Y. Shimizu, M. Egashira, Gas sensing properties of ordered mesoporous SnO_2 and effects of coatings thereof, Sens. Actuators B 93 (2003) 590-600.
5. T. Hyodo, Y. Mitsuyasu, Y. Shimizu, M. Egashira, H_2 and NOx sensing properties of ZnO and In_2O_3 powders modified with mesoporous SnO_2, J. Ceram. Soc. Jpn. 112 (2004) S540-545.
6. Y. Shimizu, K. Tsumura, T. Hyodo, M. Egashira, Effect of simultaneous modification with metal loading and mesoporous layer on H_2 sensing properties of SnO_2 thick film sensors, IEEJ Trans. SM 125 (2005) 70-74.
7. Y. Shimizu, E. Di Bartolomeo, E. Traversa, G. Gusmano, T. Hyodo, K. Wada, M. Egashira, Effect of surface modification on NO_2 sensing properties of SnO_2 varistor-type sensors, Sens. Actuators B 60 (1999) 118-124.

8. K. Wada, M. Egashira, Hydrogen sensing properties of SnO_2 subjected to surface chemical modification with ethoxysilanes, Sens. Actuators B 62 (2000) 211-219.
9. T. Hyodo, Y. Baba, K. Wada, Y. Shimizu, M. Egashira, Hydrogen sensing properties of SnO_2 varistors loaded with SiO_2 by surface chemical modification with diethoxydimethylsilane, Sens. Actuators B 64 (2000) 175-181.
10. K. Wada, M. Egashira, Effects of Pd- and Pt-loading on the gas-sensing properties of SnO_2 subjected to surface chemical modification with diethoxydimethylsilane, T. IEE Japan 120-E (2000) 458-467.
11. Y. Shimizu, N. Kuwano, T. Hyodo, M. Egashira, High H_2 sensing performance of anodically oxidized TiO_2 film contacted with Pd, Sens. Actuators B 83 (2002) 195-201.
12. T. Iwanaga, T. Hyodo, Y. Shimizu, M. Egashira, H_2 sensing properties and mechanism of anodically oxidized TiO_2 film contacted with Pd electrode, Sens. Actuators B 93 (2003) 519-525.
13. T. Hyodo, T. Iwanaga, Y. Shimizu, M. Egashira, Effects of electrode materials and oxygen partial pressure on the hydrogen sensing properties of anodically oxidized titanium dioxide films, ITE Lett. 4 (2003) 594-597.
14. H. Miyazaki, T. Hyodo, Y. Shimizu, M. Egashira, Hydrogen sensing properties of anodically oxidized TiO_2 film sensors -effects of preparation and pretreatment conditions-, Sens. Actuators B 108 (2005) 467-472.
15. T. Kato, M. Tashiro, K. Sugimura, T. Hyodo, Y. Shimizu, M. Egashira, Preparation of hollow alumina microspheres by ultrasonic spray pyrolysis, J. Ceram. Soc. Jpn 110 (2002) 146-148.
16. M. Egashira, T. Kato, T. Hyodo, Y. Shimizu, Preparation of hollow alumina microspheres by mechanofusion and ultrasonic spray pyrolysis, Key Eng. Mater. 247 (2003) 427-432.
17. F. Iskandar, Mikrajuddin, K. Okuyama, In situ production of spherical silica particles containing self-organized mesopores, Nano Lett. 1 (2001) 231-234.
18. F. Iskandar, Mikrajuddin, K. Okuyama, Controllability of pore size and porosity on self-organized porous silica particles, Nano Lett. 2 (2002) 389-392.
19. T. Hyodo, K. Sasahara, Y. Shimizu, M. Egashira, Preparation of macroporous SnO_2 films using PMMA microspheres and their sensing properties to NO_x and H_2, Sens. Actuators B 106 (2005) 580-590.
20. T. Ishibashi, T. Hyodo, Y. Shimizu, M. Egashira, Preparation of macroporous SnO_2 thick films and their application to sensor materials, Chemical Sensors VI, The Electrochem. Soc. 8 (2004) 28-35.
21. H. Seh, T. Hyodo, H. L. Tuller, Bulk acoustic wave resonator as a sensing platform for NO_x at high temperatures, Sens. Actuators B 108 (2005) 547-552.

Figure caption

Fig. 1. A schematic drawing and a photograph of a feeding system of a precursor solution atomized by ultrasonication.

Fig. 2. XRD patterns of pr-SnO_2(d)T (T = 800~1100) and pr-SnO_2(t)1100.

Fig. 3. TEM images of various porous SnO_2 particles, a~e: low magnification and a'~e': high magnification. a and a': pr-SnO_2(d)800, b and b': pr-SnO_2(d)900, c and c': pr-SnO_2(d)1000, d and d': pr-SnO_2(d)1100, e and e': pr-SnO_2(t)1100.

Fig. 4. Pore size distributions of pr-SnO_2(d)T (T = 800~1100), pr-SnO_2(t)1100 and c-SnO_2.

Fig. 5. SEM images of thick film pr-SnO_2(n)1100 (n: d and t) sensors.

Fig. 6. Response transients of thick film pr-SnO_2(d)1100 and c-SnO_2 sensors to 1000 ppm H_2 at 300°C.

Fig. 7. Temperature dependence of response of thick film pr-SnO_2(d)T (T = 800~1100) and c-SnO_2 sensors to 1000 ppm H_2 balanced with air.

Fig. 8. Response transients of thick film pr-Sb/SnO_2(n)1100 (n: d and t) sensors to 1000 ppm H_2 at 300°C.

Fig. 9. Temperature dependence of response of thick film pr-Sb/SnO_2(n)1100 (n: d and t) and c-SnO_2 sensors to 1000 ppm H_2 balanced with air.

Biographies of authors

Koji Hieda received his B. Eng. Degree in materials science and engineering in 2006 from Nagasaki University. He is now a student in Graduate School of Science and Technology, Nagasaki University, and is currently engaged in research and development of an adsorption/combustion-type sensor.

Takeo Hyodo received his B Eng Degree in applied chemistry and M Eng Degree in materials science and technology in 1992 and 1994, respectively, and Dr Eng Degree in 1997 from Kyushu University. He has been a research associate at Nagasaki University since 1997. His current interests are the development of electrochemical devices such as chemical sensors and lithium batteries, and mesoporous and macroporous materials.

Yasuhiro Shimizu received his B Eng Degree in applied chemistry in 1980 and Dr Eng Degree in 1987 from Kyushu University. He has been a professor at Nagasaki University since 2005. His current research concentrates on design of intelligent sensors by controlling gas diffusivity and reactivity, development of new sensor materials.

Makoto Egashira received his B Eng Degree and M Eng Degree in applied chemistry in 1966 and 1968, respectively, and Dr Eng Degree in 1974 from Kyushu University. He has been a professor at Nagasaki University since 1985. His current interests include the development of new chemical sensors and surface modification of ceramics, preparation of hollow ceramic microspheres and porous films.

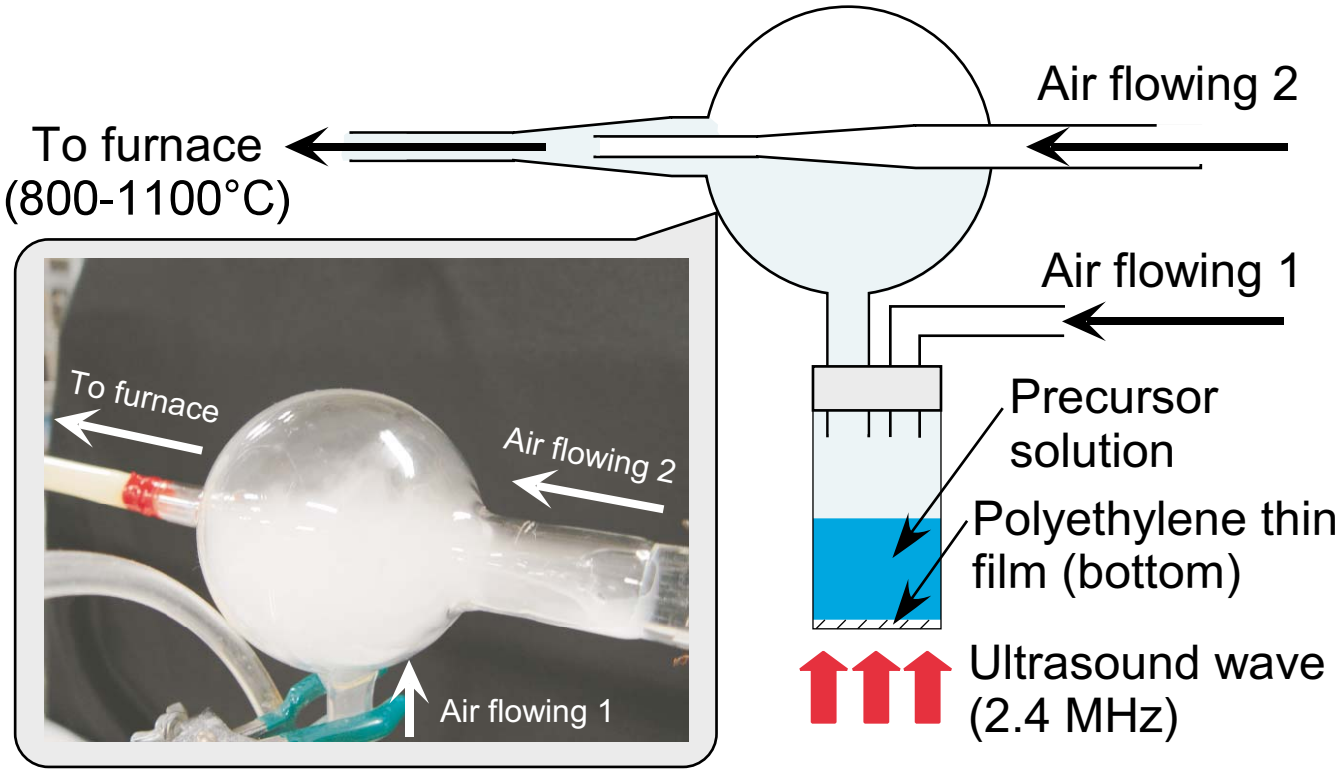

Fig. 1. Hieda et al.

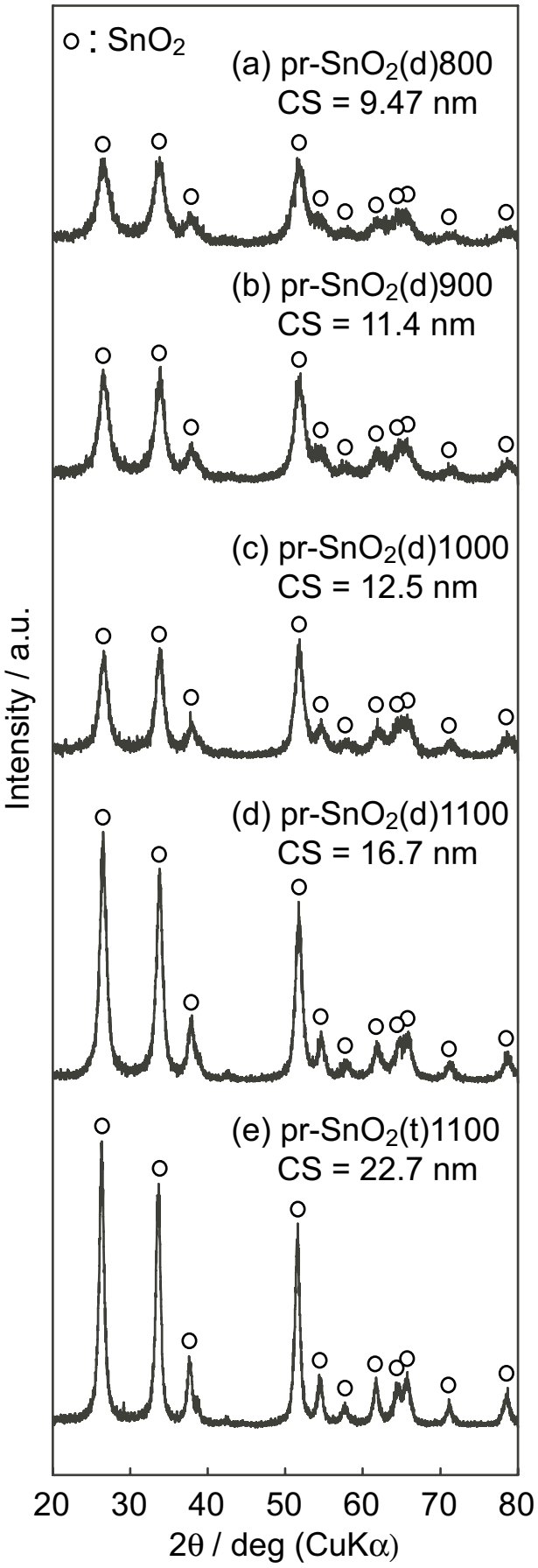

Fig. 2. Hieda et al.

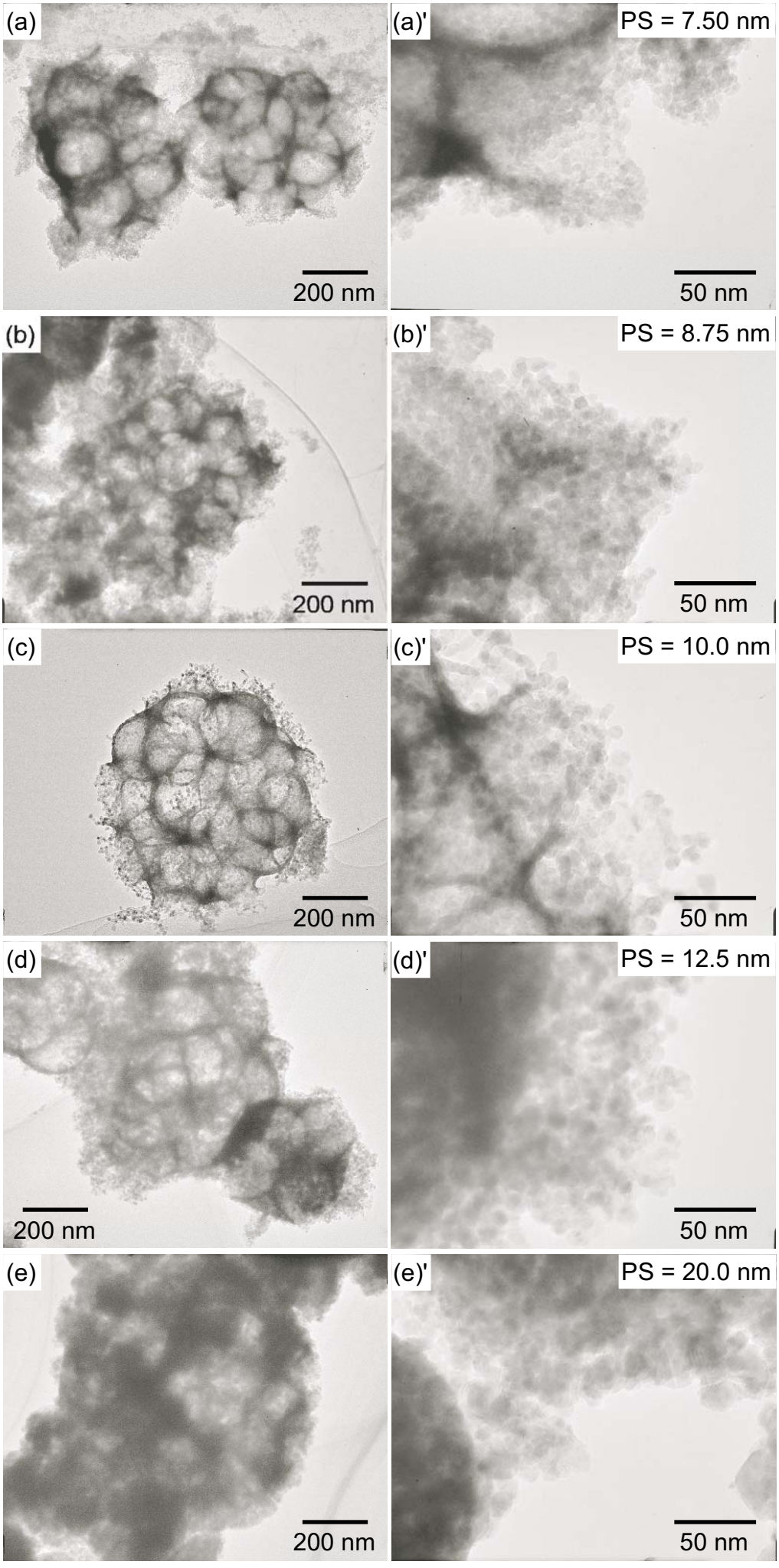

Fig. 3. Hieda et al.

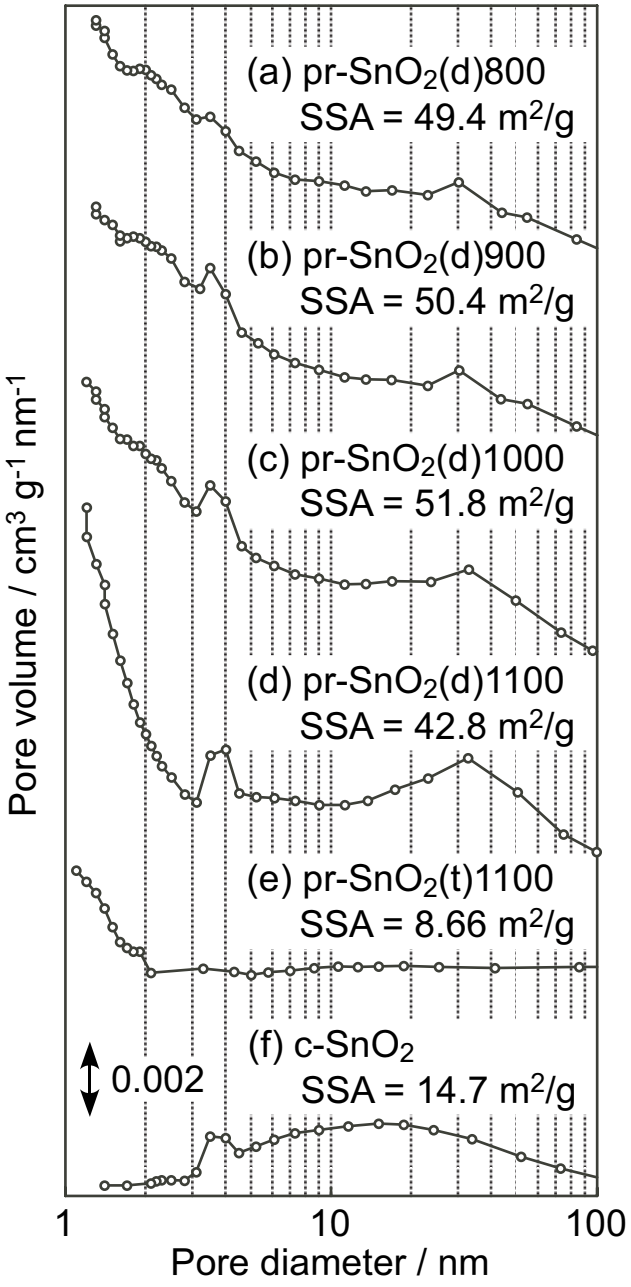

Fig. 4. Hieda et al.

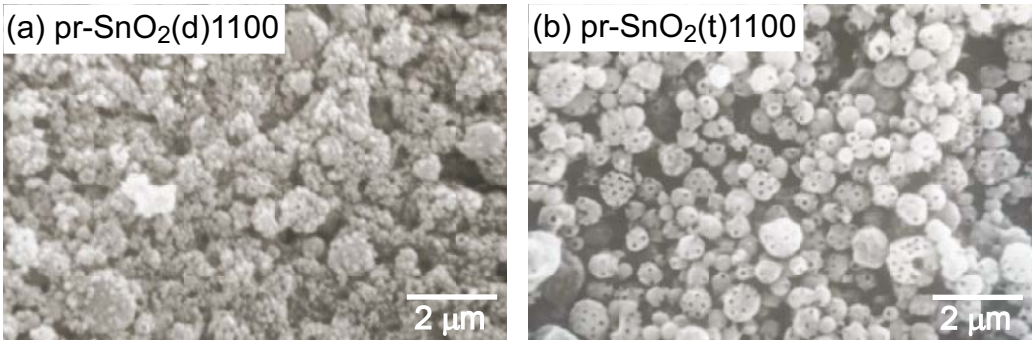

Fig. 5. Hieda et al.

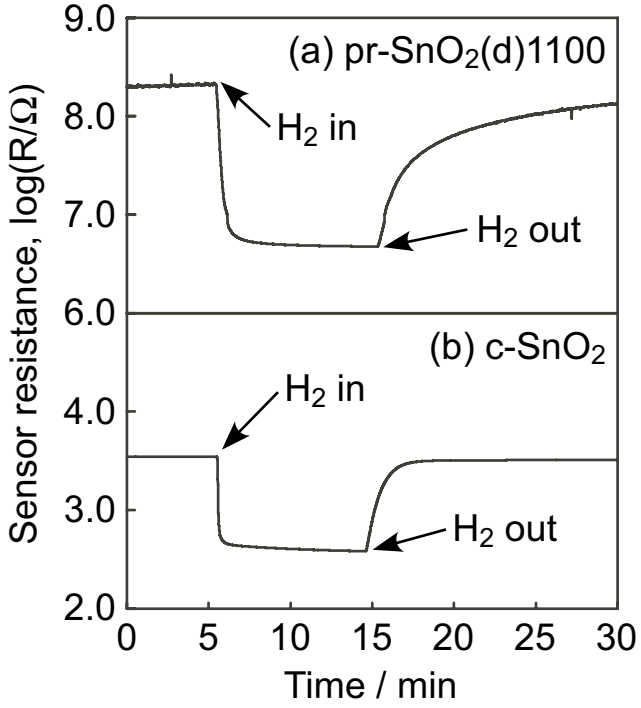

Fig. 6. Hieda et al.

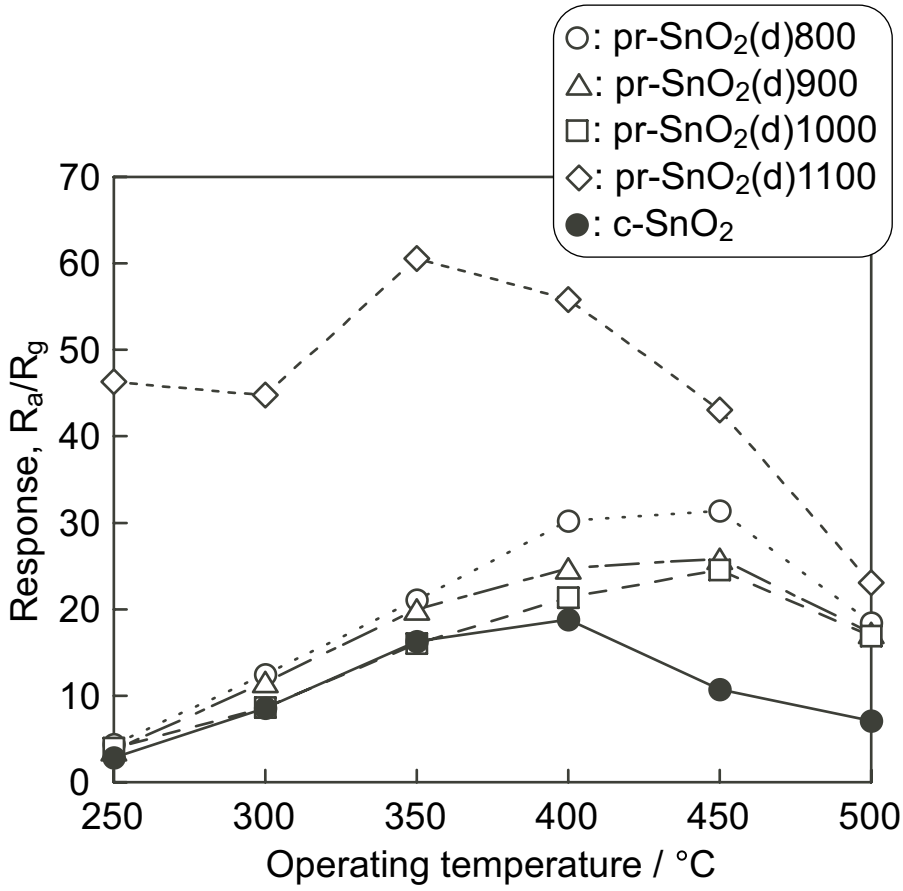

Fig. 7. Hieda et al.

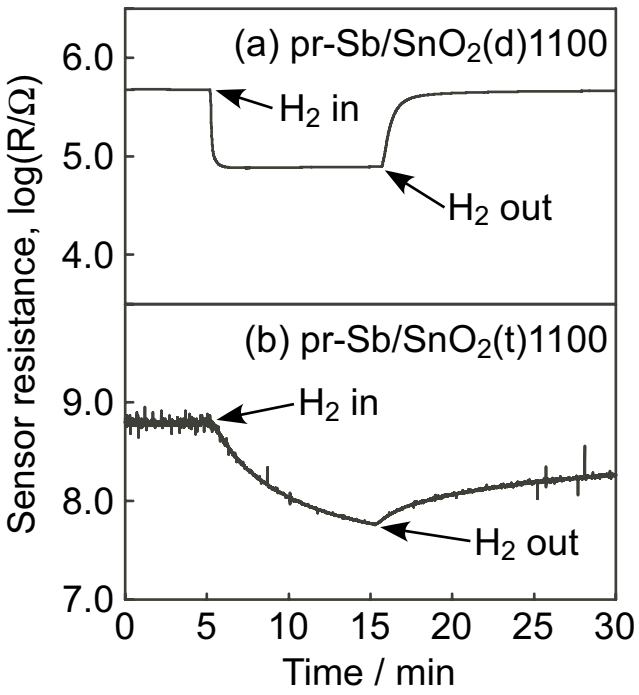

Fig. 8. Hieda et al.

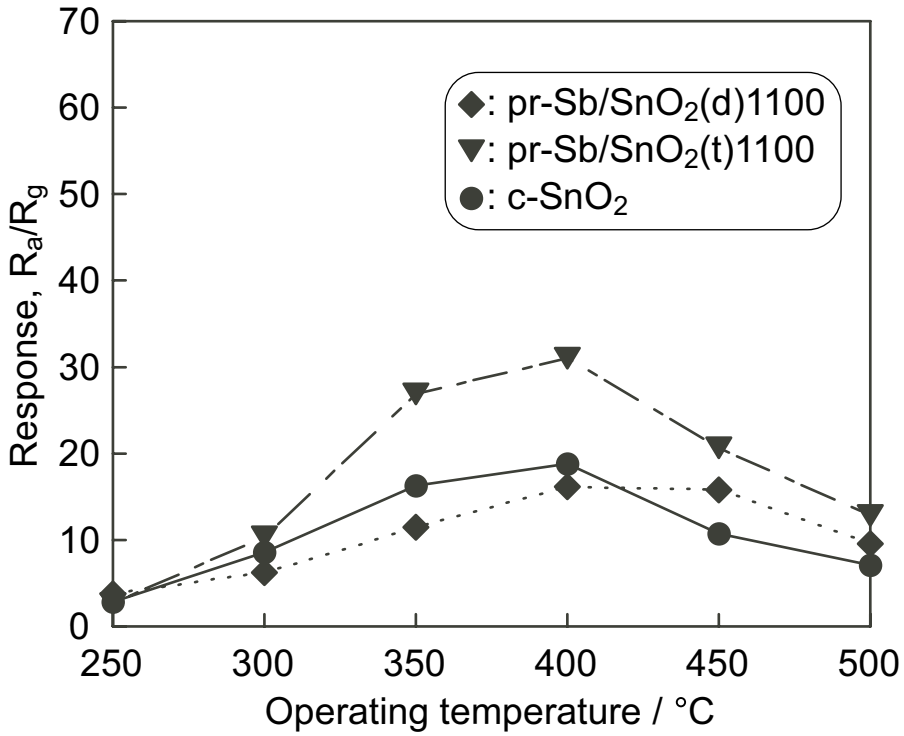

Fig. 9. Hieda et al.